147 (2023) 213331

Contents lists available at ScienceDirect

Biomaterials Advances

journal homepage: www.journals.elsevier.com/materials-science-and-engineering-c

Biomimetic polyelectrolyte coating of stem cells suppresses thrombotic activation and enhances its survival and function

Vignesh K. Rangasami [a,f], Kenta Asawa [b], Yuji Teramura [c], Katrina Le Blanc [d], Bo Nilsson [e], Jöns Hilborn [f], Oommen P. Varghese [f], Oommen P. Oommen [a,*]

[a] Bioengineering and Nanomedicine Group, Faculty of Medicine and Health Technologies, Tampere University, 33720 Tampere, Finland
[b] Department of Bioengineering, The University of Tokyo, 7-3-1 Hongo, Bunkyo-ku, Tokyo 113-8656, Japan
[c] Cellular and Molecular Biotechnology Research Institute (CMB), National Institute of Advanced Industrial Science and Technology (AIST), Tsukuba Central Fifth, 1-1-1 Higashi, Tsukuba, Ibaraki 305-8565, Japan
[d] H5 Department of Laboratory Medicine, Karolinska Institute, Stockholm, Sweden
[e] Department of Immunology, Genetics and Pathology, Rudbeck Laboratory, Uppsala University, SE-75105, Sweden
[f] Macromolecular Chemistry, Department of Chemistry - Ångström Laboratory, Uppsala University, 751 21 Uppsala, Sweden

ARTICLE INFO

Keywords:
Mesenchymal stem cells
Cell therapy
Heparin
Thrombosis
Layer-by-layer coating

ABSTRACT

Mesenchymal stem cells (MSCs) therapy is a promising approach for treating inflammatory diseases due to their immunosuppressive and tissue repair characteristics. However, allogenic transplantation of MSCs induces thrombotic complications in some patients which limits its potential for clinical translation. To address this challenge, we have exploited the bioactivity of heparin, a well-known anticoagulant and immunosuppressive polysaccharide that is widely used in clinics. We have developed a smart layer-by-layer (LbL) coating strategy using gelatin and heparin polymers exploiting their overall positive and negative charges that enabled efficient complexation with the MSCs' glycocalyx. The stable coating of MSCs suppressed complement attack and mitigated thrombotic activation as demonstrated in human whole blood. Gratifyingly, the MSC coating retained its immunosuppressive properties and differentiation potential when exposed to inflammatory conditions and differentiation factors. We believe the simple coating procedure of MSCs will increase allogenic tolerance and circumvent the major challenge of MSCs transplantation.

1. Introduction

Over the past few decades, there has been an exponential growth in stem cell research, owing to their unique immunosuppressive characteristics and broad differentiation potential. Stem cells have revolutionized the field of biomedicine and have made a momentous impact on our approach to treating a range of diseases. Among different types of stem cells, human embryonic stem cells are the most pluripotent which could be differentiated into a wide range of cell types. However, it could not be used to its full potential owing to ethical concerns surrounding their use [1]. The somatic or adult stem cells, such as mesenchymal stem/stromal cells (MSCs) though not as potent as the embryonic stem cells, are identified as an ideal replacement as there are less stringent ethical concerns to its isolation and use and are exploited for treating a broad range of diseases and regenerative medicine applications [2]. Despite its phenomenal success in the clinic, MSC transplantation and therapy has suffered from adverse pro-thrombotic activity and poor in-vivo survival. Intravenous administration of MSCs has been reported to cause pulmonary embolism in mice due to its procoagulant properties resulting in higher accumulation in the lungs when compared to the target site [3]. Such thrombotic activity, mediated by the instant blood mediated inflammatory reaction (IBMIR) has caused serious concerns about its safety with incidences of death in some patients [4]. In addition to pulmonary embolism, allograft tolerance after MSCs implantation is another challenge as the implanted MSCs get injured after infusion by the complement attack [5]. To overcome this problem, we have designed a pluronic micelles-based siRNA delivery system that efficiently silenced tissue-factor gene that suppressed coagulation cascade which significantly improved its survival in human blood and enhanced its paracrine signaling and differentiation potential [6]. Other strategies such as grafting heparin-binding peptides [7,8] or cell-penetrating peptides on the cell surface [9], using PEG phospholipid construct

* Corresponding author.
E-mail address: oommen.oommen@tuni.fi (O.P. Oommen).

https://doi.org/10.1016/j.bioadv.2023.213331
Received 25 August 2022; Received in revised form 12 January 2023; Accepted 5 February 2023
Available online 8 February 2023

conjugation of nanogels on the cell surface [10], using synthetic polymers in combination with natural polymers [11], using photo cross-linking methods to coat the cells [12], using lipids conjugated heparin [13] have been successfully studied. A multifaceted approach of coating the cells with lipids conjugated with a peptide and enzyme that could regulate the complement and coagulation has also been studied successfully [14]. All these successful methods require complex synthesis steps, either fabricating lipids or nanoparticles or synthesizing peptides and conjugating them to lipids or exposing the cells to blue light. These steps could be a hindrance in the translation from bench to clinic.

Lately, layer-by-layer (LbL) self-assembly of polymers has been developed as a versatile engineering strategy where polymers of opposite charges are coated on biomaterials and living cells to form a nanosized multilayer biofilm which enhances the biocompatibility and functionality of encapsulated cells and biomaterials [15]. The single-cell encapsulation by LbL biofilm of nanoscale thickness protects the cells from physical damage caused during transplantation and provides a conducive microenvironment for cell integration. The success of LbL coating depends on the cationic and anionic charges of the polymer used. Since cell surface is largely anionic due to the presence of sialic acid and other glycosaminoglycans, the ionic pair of cationic gelatin and anionic alginate is most widely used to coat stem cells [16,17]. Other examples involve gelatin-coating followed by a layer of fibronectin, which was further encapsulated in a microgel and used in a microfluidic device to fabricate cardiac tissue [18]. Although, the LbL strategy of using alginate and gelatin has immensely helped in cell engineering, by improving the survival, proliferation, differentiation, and also as a reservoir for growth factor delivery, the pro-coagulant nature of the coating hampers its clinical use [19]. Thus, there is a pressing need to develop new cell engineering strategies, that not only provide enhanced stability and protect against anoikis but also prevent activation of coagulation cascade while retaining the paracrine activities and differentiation potential.

Here, in this study, we have devised a simple strategy where we coat the MSCs with polymers to help evade the immune system and reduce the procoagulant properties of the MSCs. We have used gelatin and heparin as the two different polymers with which we coated the cells. The cells were coated with these polymers following an LbL approach such that there were two layers of gelatin (G) and two layers of heparin (H). We found that the polyelectrolyte coating of the MSCs suppressed pro-procoagulant activity in human whole blood and enhanced proliferative activity while retaining the paracrine signaling and differentiation potential of these MSCs.

2. Materials and methods

2.1. Coating solutions preparation

Heparin (H) (Sigma Aldrich, H3393-500KU) 1 % wt/vol was prepared by dissolving the desired amount of heparin in a serum-free cell culture medium and 0.1 % wt/vol gelatin type-A (G) (Sigma Aldrich, G2625) solution was prepared separately by dissolving gelatin in the Dulbecco's phosphate-buffered saline (DPBS) (Gibco, 14190169). The heparin solution was filter sterilized using 0.22 μm filters, while the gelatin solution was autoclaved before use.

2.2. Coating of the cells

Human bone marrow-derived mesenchymal stromal cells (hMSCs) (from 5 different donors) in passage four were cultured in α-MEM (Gibco, 32561037) supplemented with 10 % FBS, 1 % L-glutamine, and 1 % penicillin/streptomycin (Sigma P4333) and were harvested when reached to 60–80 % confluency using the trypsin-EDTA solution. Approximately, 2×10^6 cells were resuspended in 1 mL of gelatin solution and incubated for 10 min under mild shaking. Cells were centrifuged at 500*g* for 5 min and re-suspended in the heparin solution and incubated for 10 min under mild shaking. The two previous steps were repeated alternatively until the cells were coated with four layers of the polymers as schematically expressed in Fig. 1A. Ethical approval was obtained from the Local Ethics Committee, Stockholm, and all the donors provided written consent (DNR 2010/1650 and DNR 2014/51432).

2.3. Proliferation of the cells

Cellular proliferation was measured by AlamarBlue® assay (Fisher Scientific 10099022). H/G coated MSCs (c-MSCs) and uncoated cells (C) as control group was seeded in 5000 cells in tissue culture 96 well plates. After 24 h of culturing the cells, all wells were washed with pre-warmed DPBS once to remove the free growth factor, and then, the serum-free culture media without any growth factors was added to the wells. Cellular proliferation was measured at each time point by reading the fluorescent intensity at 590 nm using a plate reader (Infinite 200 pro Tecan). For AlamarBlue® assay, the reagent was added to the cells after aspirating the medium and washing cells with pre-warmed DPBS for one time. The cells were incubated for 2 h at 37 °C and 5 % CO_2. Then, samples were read at 590 nm using plate reader model Infinite 200 pro Tecan.

2.4. Human whole blood compatibility assay

Blood was obtained from healthy volunteers who had received no medication for at least 10 days prior to blood donation. MSCs or coated MSCs (c-MSCs) in passage 4 were cultured and coated with gelatin and heparin. The two groups were exposed to human blood using the Chandler loop model. The blood-collection materials were coated with heparin according to the manufacturer's instructions (Corline AB). Whole blood from healthy donors was collected into heparin conjugate-coated PVC tubes without any anticoagulants. Then, 3 mL of human blood were added to prepared tubing loops and supplemented with 100 μL of PBS containing MSCs or c-MSCs (1.5×10^4 cells/mL), prepared as described in the previous section. The tubes were rotated vertically at 30 rpm for 60 min in a 37 °C cabinet. Then, 1.2 mL of blood was collected from each tube and mixed with 2,2′,2″,2‴-(ethane-1,2-diyldinitrilo)tetra acetic acid (EDTA)-K3 solution at a final concentration of 10 mM, and the platelet concentration was analyzed in a Coulter AcT 5diff® hematology analyzer (Coulter Corporation, Miami, FL, USA). The blood was then centrifuged at 4200*g* for 15 min at 4 °C, and the plasma was collected and stored at −80 °C until further analysis by enzyme immunoassay (EIA) for C3a, sC5b-9, and TAT. Ethical approval was obtained from the regional ethics committee in Uppsala (#2008-264).

2.5. Measurement of C3a, sC5b-9, and TAT in plasma

Conventional sandwich ELISA was used to measure the C3a, sC5b-9, and TAT in plasma. For soluble C3a, plasma was diluted in a working buffer (PBS containing 0.05 % Tween 20, 10 mg/mL BSA, and 10 mM EDTA). As previously reported, C3a was captured by anti-human C3a mAb 4SD17.3 and detected by a biotinylated polyclonal rabbit anti-C3a antibody and horseradish peroxidase (HRP)-conjugated streptavidin. Zymosan-activated serum, calibrated against purified C3a, served as a standard. Values are expressed as ng/mL. For sC5b-9, plasma was diluted in a working buffer. sC5b-9 was captured by anti-human C5b-9 mAb aE11 (Diatec Monoclonal AS, Oslo, Norway) and detected with anti-human C5 polyclonal rabbit antibody (Dako) and HRP-conjugated anti-rabbit IgG (Dako). Zymosan-activated serum served as a standard. The assay was calibrated against a commercially available kit (MicroVue; Quidel Corp, Santa Clara, CA, USA), and values are expressed as ng/mL. For TAT, plasma was diluted in normal citrate-phosphate-dextrose plasma. TAT was captured by anti-human thrombin mAb and detected by an HRP-coupled anti-human AT mAb (Enzyme Research Laboratories, South Bend, IN, USA). A standard prepared by diluting pooled human serum in normal citrate-phosphate-dextrose plasma was

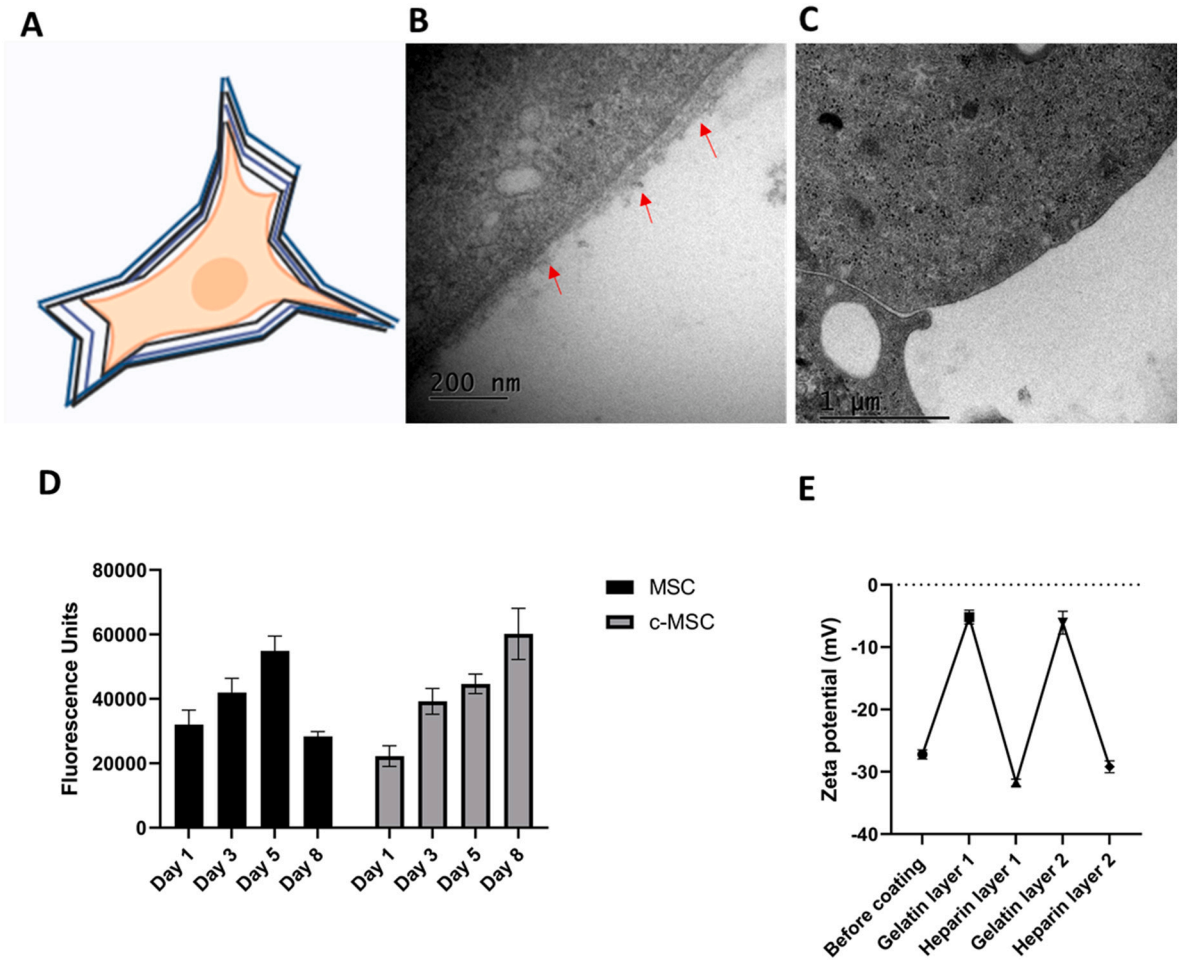

Fig. 1. (A) Schematic representation of the coated MSCs (c-MSCs) with the four alternating layers of heparin (blue) and gelatin (black). Transmission electron microscopy images of (B) c-MSCs and (C) MSCs. The red arrows depict the presence of coating in c-MSCs and the absence of coating in MSCs. (D) Alamar blue proliferation assay was performed on the MSCs and c-MSCs at different timepoints depicting the proliferation rates (N = 6). (E) Zeta potential reading was observed after each layer of coating of the cells with H/G coating (N = 3).

used. Values are expressed as µg/L.

2.6. Evaluation of cytokine release

Briefly, 50,000 cells (c-MSCs and uncoated MSCs) were plated in 24 well plates and cultured for three days and seven days in the conditions mentioned earlier. For the stimulated groups, the cells were stimulated with IFNγ (100 U/mL) and TNFα (10 ng/mL). For the protein level cytokine analysis of IL6 and IL8, human IL6 DuoSet ELISA kit (DY206) and human IL8 DuoSet ELISA kit (DY208) were obtained from R&D Systems (Biotechne). The manufacturer's protocols were followed for the experiments. For mRNA level analysis, at the respective time points, the RNA from the cells were extracted using the RNeasy Mini kit (Qiagen). The cDNA was then prepared using the Maxima first-strand cDNA kit (Thermofisher) according to the manufacturer's protocol. The qRT-PCR was performed with cDNA and TaqMan Fast advanced master mix (Thermofisher). TaqMan primer assays for *il6*, *il8*, *tnf*, *vegf*, *hif1* and *actb* were obtained from Thermofisher. The amplification was done using a Bio-Rad CFX1000 instrument following a 40-cycle program. Samples were normalized relative to *actb* and gene expression analysis was done following the 2−ΔΔCT method.

2.7. Effect of conditioned medium on C28/I2 chondrocytes and THP1 cells

THP-1 cells, a human leukemia monocytic cell line was cultured in RPMI (Gibco, 21875034) with 10 % FBS and 1 % penicillin-streptomycin at 37 °C and 5 % CO_2. Briefly, THP-1 one cells were differentiated with 50 ng/mL phorbol myristic acid (PMA; Sigma, P8139) for 24 h at 37 °C and 5 % CO_2. The cells were then treated with 500 ng/mL lipopolysaccharide (Sigma) for 24 h at 37 °C and 5 % CO_2 to make them M1 macrophage-like. The conditioned medium (after 7 days) from the coated MSCs and uncoated MSCs were exposed to the M1 polarized THP1 cells. The M1 like THP-1 cells were incubated in these conditions for a period of 3 days after which this medium was collected and analyzed by the multiplex bead-based assay as mentioned below.

Protein level analyses were done with the detection of cytokines from the medium. A bead-based cytokine detection immunoassay from LEGENDplex (BioLegend, Nordic Biosite, 740509) was used to identify the secreted cytokines following in-vitro cell culture. The cell culture supernatants were collected at the respective time points and stored at −80 °C before use. The human macrophage/microglia cytokine panel was used, and the assays were performed following the manufacturer's protocol. The analysis was done using the LEGENDplex data analysis software (BioLegend) and the cytokines were quantified by comparing samples to a set of standards.

Human chondrocytes (C28/I2) cells were cultured in DMEM (Gibco,

10565018) with F12 nutrients, 10 % FBS, and 1 % penicillin-streptomycin at 37 °C and 5 % CO_2. LPS (1 μg/mL) was used added to the medium to stimulate the chondrocytes for 24 h. Briefly, 35,000 C28/I2 cells were plated and cultured overnight at the conditions mentioned above. These cells were then stimulated with LPS for another 24 h after which the conditioned medium from the c-MSC and uncoated MSCs were added to these cells and were cultured for a further 48 h. RNA was then isolated using the RNeasy Mini kit (Qiagen). The cDNA was then prepared using the Maxima first-strand cDNA kit (Thermofisher) according to the manufacturer's protocol. The qRT-PCR was performed with cDNA and TaqMan Fast advanced master mix (Thermofisher). TaqMan primer assays for *tnf*, *tgfβ*, *il1β* and *actb* were obtained from Thermofisher. The amplification was done using a Bio-Rad CFX1000 instrument following a 40-cycle program. Samples were normalized relative to *actb*, and gene expression analysis was done following the 2−ΔΔCT method.

2.8. Osteogenic and adipogenic differentiation of the c-MSCs

In order to investigate if c-MSCs differentiate into different lineages, an osteogenic and adipogenic differentiation had been carried out in both c-MSCs and uncoated cells as a control group using StemPro® Osteogenesis (Gibco, Thermofisher, A1007201) and Adipogenesis Differentiation Kits (Gibco, Thermofisher, A1007001), respectively as per manufacturer's instructions. Briefly, the cells were seeded in 24-well plates for osteogenic and adipogenic differentiation, respectively. Cells were incubated with prewarmed MSC growth medium at 37 ° C and 5 % CO_2 overnight and then the medium was changed either with Complete Osteogenesis or Adipogenesis differentiation medium and cultures refed every 3 days. After 14 days, Alizarin red S (Sigma) and Oil Red O (ChemCruz, Santa Cruz Biotechnology) staining were carried out to confirm osteogenic and adipogenic differentiation. Briefly, for the osteogenic differentiation, the cells were fixed with 4 % paraformaldehyde for 15 min. The cells were then washed 3 times with PBS and then stained with 2 % Alizarin red solution for 10 min. The samples were then washed 3 times with distilled water and observed under the microscope. For the adipogenic differentiation, of the cells, the cells were again fixed with 4 % paraformaldehyde and incubated for 15 min. The cells were then washed with distilled water (twice) and then 60 % isopropanol was added just enough to cover the cells completely. The cells were incubated for 5 min in 60 % isopropanol after which oil red o working solution is added and incubated for 10–20 min. The cells were then washed with distilled water 4–5 times until no excess stain is seen. The cells were then covered with water and then observed under the microscope (Nikon). For, the qRT-PCR, the RNA from the cells was extracted using the RNeasy Mini kit (Qiagen). The cDNA was then prepared using the Maxima first-strand cDNA kit (Thermofisher) according to the manufacturer's protocol. The qRT-PCR was performed with cDNA and TaqMan Fast advanced master mix (Thermofisher). TaqMan primer assays for *alpl*, *bglap*, *lpl*, *pparg* and *actb* were obtained from Thermofisher. The amplification was done using a Bio-Rad CFX1000 instrument following a 40-cycle program. Samples were normalized relative to *actb* and gene expression analysis was done following the 2−ΔΔCT method.

2.9. Statistics

The statistical measurements were achieved by comparing each experimental value with their respective controls or groups. The assessments between the two groups were performed using the ANOVA and Mann Whitney test as indicated. These tests were performed using GraphPad Prism Software *$P < 0.05$ was the statistical significance for all tests.

3. Results and discussion

3.1. Encapsulation of MSCs with polyelectrolyte coatings

Herein, we encapsulated MSCs within a stable polyelectrolyte coating that consisted of two different polymers namely, heparin and gelatin. The cells were first coated with positively charged gelatin that would neutralize the net negative charge on the cell surface forming a stabilized coat. The gelatin layer could then be coated with negatively charged heparin polymer forming a stable nanocapsule around the stem cells. The choice of gelatin and heparin offers great advantages as they are natural biopolymers that are biocompatible and possess diverse bioactivities. The gelatin-based biomaterial scaffolds are widely used for tissue engineering applications, especially for designing bioinks for 3D bioprinting [20]. Hydrogels designed using gelatin derivatives display immunomodulatory properties and have been shown to suppress inflammation when tested in inflamed conditions [21]. Heparin, on the other hand, is a glycosaminoglycan that possesses immunosuppressive characteristics and is used in clinics as an anti-coagulant. Heparin is a highly sulphated glycosaminoglycan that binds to several biological molecules such as cytokines and growth factors [22]. It is also known for its anti-inflammatory property by inhibiting the activity of the various immune cells [23–25] suppressing the ability of the neutrophils to activate the platelets [26] and also assisting in tissue regeneration and wound healing [27]. Recently, heparin-based nanoparticles have also been known to cross the blood-brain barrier and target the implanted tumor in mice models [28]. We anticipated that the outer coat of heparin on the MSCs cell surface would protect the cells from complement attack and provide stealth properties, thus mitigating IBMIR and subsequent immune rejection, which is the major challenge of cell-based therapies.

To establish a stable coating of the cells, we decided to use two layers of gelatin and heparin (altogether four layers) that would render enhanced stability. To confirm the efficient coating of the polyelectrolyte layers, we estimated the charge on the cell surface after each coating step by measuring the zeta potential of the coated cells using zeta sizer. As expected, the surface charge of the cells without any coating was found to be $\sim -27.2 \pm 0.8$ mV. The addition of the first coat of gelatin neutralized the surface charge of the cells to $\sim -5.2 \pm 1.1$ mV confirming the complexation (resulting in charge neutralization) between the two polymers (Fig. 1E). The gelatin-coated cells were then treated with heparin polymer that changes the surface charge of the cells to $\sim -31.7 \pm 0.6$ mV. Subsequent treatment of the coated cells with another layer of gelatin and heparin rendered the net cell surface charge of $\sim -6.1 \pm 1.8$ mV and $\sim -29.2 \pm 1$ mV respectively, indicating successful heparin-gelatin polyelectrolyte coating (H/G) on the MSCs (c-MSCs). To further confirm the successful coating and persistence of the layers under cell culture conditions, we performed transmission electron microscopy (TEM) analysis of the c-MSCs and control MSCs after 3 days of culture. Gratifyingly, we observed nanosized coating of the polyelectrolyte layers in c-MSCs which were absent in control MSCs (Fig. 1B & C). The heparin and gelatin coats could be degraded ubiquitously by the enzymes such as heparanase, and collagenase, respectively that are abundantly found in inflamed tissues and extracellular matrix [29–31]. However, we believe the coating on the cells would have sufficient half-life, as recently it was reported that heparin coated iron oxide particles displayed high circulation in blood up to a period of 14 days [32].

After validating the successful encapsulation of MSCs within polyelectrolyte H/G coating, we examined if the MSC coating influences cell proliferation rate. We performed an Alamar Blue assay and estimated the cell proliferation for a period of 8 days. We observed that the c-MSCs and control MSCs show good proliferation up to day 5, albeit with a lower rate for c-MSCs. However, unlike c-MSCs, the proliferation of control MSCs drastically slowed down after day 5, while the c-MSCs continued proliferation (Fig. 1D). We believe this enhanced proliferation by the coated cells is attributed to the heparin and gelatin polymers that are known to accelerate stem cell proliferation [33,34]. However, as we

observed a drastic increase in the proliferation rates of the c-MSCs after day 5, we further examined the proliferation rate with MTS based assay (Fig. S1 in Supporting information). Interestingly, the MTS assay also revealed that the coating of the cells did not hinder the proliferation rates of the c-MSCs. It was also observed that the c-MSCs had a marginally higher proliferation rates compared to the MSCs suggesting that the coating can indeed be beneficial to the growth rates of the cells.

3.2. Hematological evaluation of c-MSCs

To access if the c-MSCs are protected from complement attack and do not trigger IBMIR, we investigated the effect of the c-MSCs and uncoated MSCs on fresh non-anticoagulated human whole blood (i.e., whole blood that was not treated with any anticoagulants). For this purpose, c-MSCs and MSCs were incubated in a modified chandler's loop with non-anticoagulated human whole blood for 1 h. We found that poly-electrolyte coating of MSCs (c-MSCs) attenuated the platelet aggregation as we observed ~94 % free platelets in the c-MSC group while only ~2 % of platelets were found in the control MSCs group (Fig. 2A). These observations were further corroborated with the TAT complex representing activation of the coagulation cascade, which were significantly lower in the c-MSCs when compared to the control MSC group (Fig. 2B).

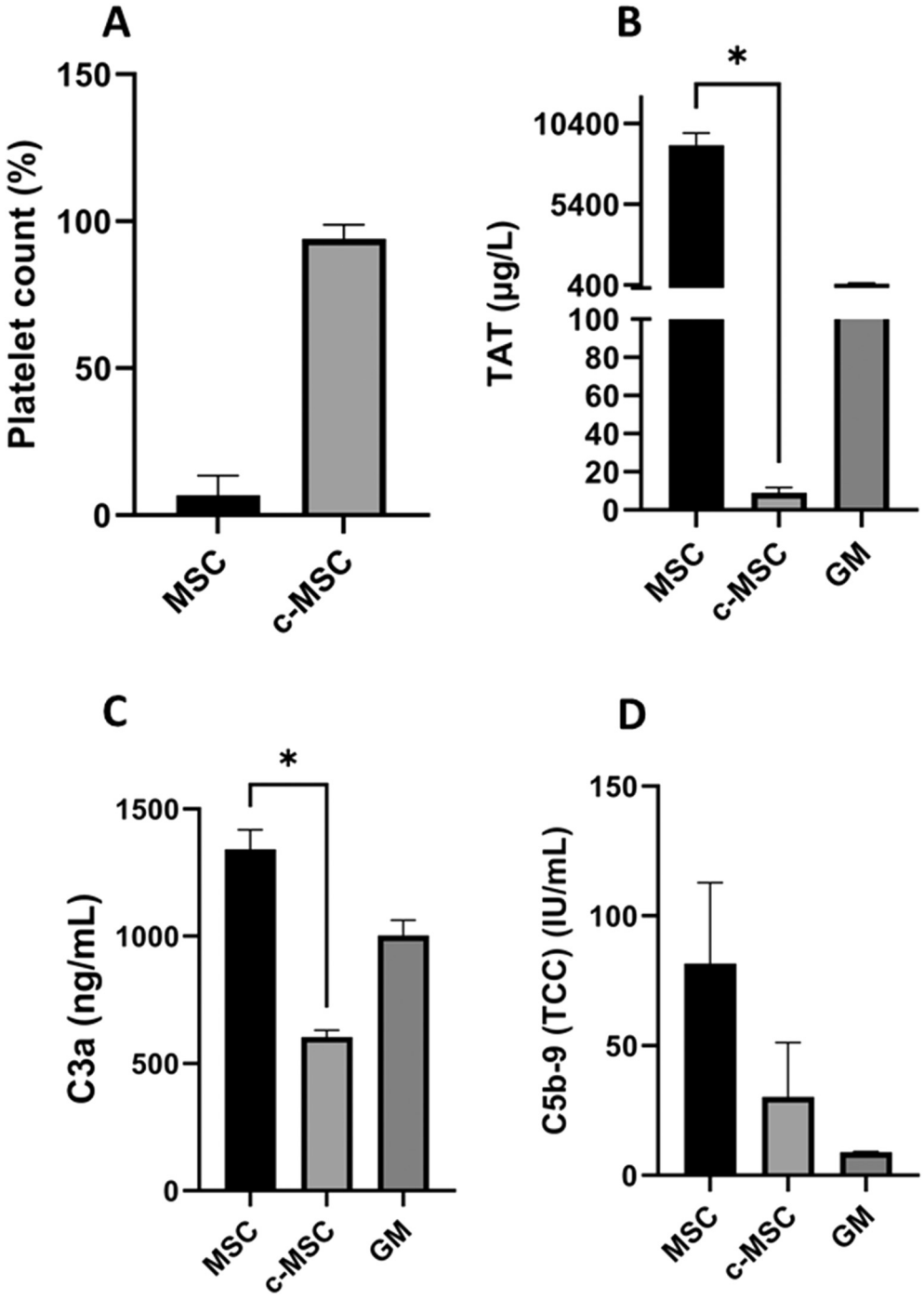

Fig. 2. (A) Platelet counts observed after incubation of c-MSCs and MSCs in non-anticoagulated blood, normalized against the growth medium (GM). (B) TAT complex, a marker for coagulation in whole blood (N = 3). (C, D) C3a and sC5b-9, markers for complement activation in whole blood (N = 3). Statistics were done using Mann-Whitney Test using GraphPad Prism. *P < 0.05.

Next, we investigated the effect of polyelectrolyte coating on the complement system by estimating the expression of C3a and sC5b-9 which represents the early and late markers of complement activation. As anticipated, the C3a levels in the c-MSCs were significantly lower (~600 ng/mL) when compared to the MSCs (~1300 ng/mL). The C5b-9 marker levels were lower in the c-MSCs (~30 IU/mL) when compared to the control MSCs group (~81 IU/mL), however, they were not significant (Fig. 2C, D). The reduction in the TAT generation and the complement proteins suggests that cells are well protected by the polyelectrolyte coating, which we believe is mediated by the outer layer of heparin as it is also known to suppress the activation of the complement and coagulation cascade [35,36]. This is a significant observation as c-MSCs will evade the systemic immune system and display higher cell survival after transplantation as these cells will not trigger the thromboinflammation or IBMIR in patients undergoing stem cell therapy as compared to the uncoated MSCs.

3.3. MSCs secretome and immunomodulatory properties

After establishing the stability and hemocompatibility of c-MSCs, we investigated the functional characteristics of the stem cells by estimating cytokines released by these cells. We decided to quantify the expression of IL6 and IL8 produced by the MSCs as they are key regulators of inflammation and play a crucial role in initiating the reparative process by polarizing proinflammatory M1 macrophages to a tissue regenerative M2 phenotype or indirectly stimulating wound healing [37,38]. The IL6 and IL8 cytokines also act as a chemoattractant that recruits immune cells to cartilage lesions [39] and promote cartilage regeneration in osteoarthritis [40]. We first analyzed the secretome of the c-MSCs and the uncoated MSCs obtained after three days of culture by ELISA. Interestingly, we observed that the levels of IL6 (~7 ng/mL) and IL8 (~0.13 ng/mL) secreted by the c-MSCs were much lower than the uncoated MSCs (IL6- ~17 ng/mL; IL8- ~0.9 ng/mL). Further, even after stimulation of the MSCs and c-MSCs with IFNγ and TNFα, the c-MSCs secretome produced a much lower amount of IL6 (~38 ng/mL) and IL8 (~3.7 ng/mL) after three days when compared to the stimulated MSC control (IL6- ~133 ng/mL; IL8- ~41.1 ng/mL) (Fig. 3A, B). We speculated that the factors released by the c-MSCs could adhere to the heparin in the H/G coating as heparin is known to bind cytokines, growth factors, and other biomolecules [22]. To further confirm if the c-MSCs indeed produce a lower amount of IL6 and IL8, we quantified the mRNA levels of these cytokines in the c-MSCs and control MSCs by qRT-PCR experiment. Interestingly, we observed that on day 3, the c-MSCs had significantly higher mRNA levels of *il6* and *il8* when compared to the uncoated MSCs. The polyelectrolyte-coated cells showed higher levels of *il6* and *il8* even when analyzed 7 days after culturing, though this increase was non-significant (Fig. 3C, D). We also estimated the expression of *vegf*, *hif1* and *tgfβ* (important markers for immunomodulation, tissue repair, and regeneration) as we anticipated that the nanocapsule formed around the c-MSCs would insulate the cells from the surrounding milieu creating a hypoxic environment. When the mRNA levels of these markers were analyzed on day 3, we found that there were no significant differences in the mRNA levels of these markers. Intriguingly, we observed non-significant increase of the *vegf*, *hif1* and *tgfβ* mRNA levels on day 7 in c-MSCs when compared to the uncoated MSCs (Fig. 3E, F, G). The increased levels of the *hif1* could help in the survival, proliferation, and differentiation [41]. *hif1* is also known to influence the production of *vegf* [42], which is a known potent angiogenic factor [43]. The increase in *tgfβ* could suggest that the c-MSCs could be more efficient than the uncoated MSCs in inducing the production of regulatory T-cells that are known to partake in tissue repair and regeneration [44]. Thus, polyelectrolyte coating does not significantly reduce or inhibit the important factors released by the MSCs that are necessary for immunomodulation and tissue repair. We believe that the discrepancy in the

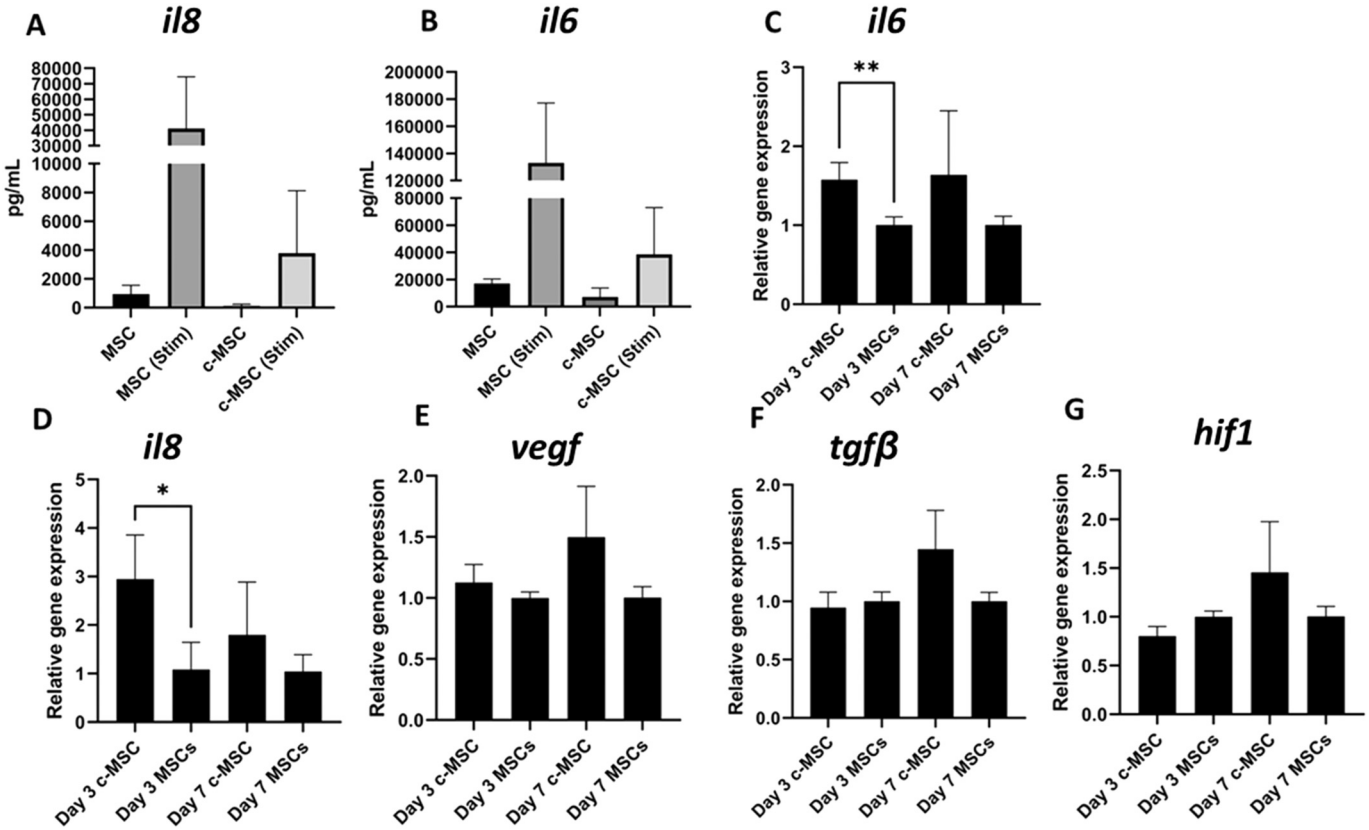

Fig. 3. (A & B) Levels of the IL8 and IL6 cytokines (in pg/mL) as analyzed through ELISA of the c-MSCs, uncoated MSCs, and c-MSCs and uncoated MSCs stimulated by IFNγ and TNFα. (C–G) mRNA expression levels of the *il6*, *il8*, *vegf*, *tgfβ* and *hif1* in uncoated and c-MSCs (n = 6). Statistics done by Anova. *P < 0.05, **P < 0.01.

ELISA and qRT-PCR data is attributed to the active sequestering of cytokines produced by the c-MSCs by the heparin coat which underestimate the cytokine concentration in the secretome, while the actual cytokine expression is better represented by the mRNA expression which is not affected by the heparin coat.

The discrepancy in the cytokine expression as determined by ELISA and the mRNA levels by qRT-PCR prompted us to investigate the paracrine signaling abilities of the c-MSCs. For this purpose, we stimulated the C28/i2 chondrocytes to a pro-inflammatory phenotype by activating them with lipopolysaccharides (LPS, 1 μg/mL) for 24 h. The conditioned medium from c-MSCs and uncoated MSCs were collected after 3 days in culture and were exposed to the stimulated chondrocytes. We analyzed the levels of the major pro-inflammatory genes *il1β* and *tnfα*. As expected, when the conditioned medium from the uncoated MSCs were incubated with the stimulated chondrocytes, we observed a decrease in *il1β* and *tnfα* mRNA expression. A similar effect was observed when the conditioned medium of the c-MSCs was used as there was a significant decline in the mRNA levels of the *il1β* and *tnfα* when compared to the LPS treated group (Fig. 4A). We also measured the levels of the anti-inflammatory marker *tgfβ* which exhibited a moderate increase in both the c-MSCs and the uncoated MSCs (Fig. 4A). These results suggest that the c-MSCs are as effective as the uncoated MSCs, and that the polyelectrolyte coating does not interfere in the paracrine signaling of the MSCs. To further confirm that the immunomodulatory properties of the MSCs are retained after the polyelectrolyte coating, we exposed the conditioned medium of the c-MSCs and uncoated MSCs to THP1 cells, that were differentiated into proinflammatory M1 like macrophages. The medium was then collected, and the cytokines expression was quantified using FACS through a multiplex bead-based assay. We specifically analyzed the proinflammatory cytokines TNFα and IL1β which are the hallmarks of pro-inflammatory macrophages. As anticipated, we saw a decrease in the production of TNFα (~274 pg/mL with CM of c-MSCs; ~611 pg/mL with CM of MSCs; and ~1410 pg/mL in control THP1) and IL1β (~70 pg/mL with CM of c-MSCs; ~95 pg/mL with CM of MSCs; and ~486 pg/mL in control THP1) when the conditioned medium of c-MSCs and control MSCs were exposed to the M1 polarized THP1 cells (Fig. 4B & C). We also estimated the expression of IP10 (CXCL10), a proinflammatory cytokine that is produced by IFNγ or LPS stimulated cells [45]. We observed a drastic reduction in the production of IP10 when the conditioned medium of c-MSCs and the MSCs were exposed to the proinflammatory THP1 cells (~310 pg/mL with CM of c-MSCs; ~212 pg/mL with CM of MSCs; and ~576 pg/mL in control THP1) (Fig. 4D). The decrease in the pro-inflammatory markers released by the M1 polarized macrophages could be due to the immunosuppressive nature of the MSCs [46]. We also analyzed the levels of IL6, a pleiotropic cytokine that is known to be involved in both pro-inflammatory as well

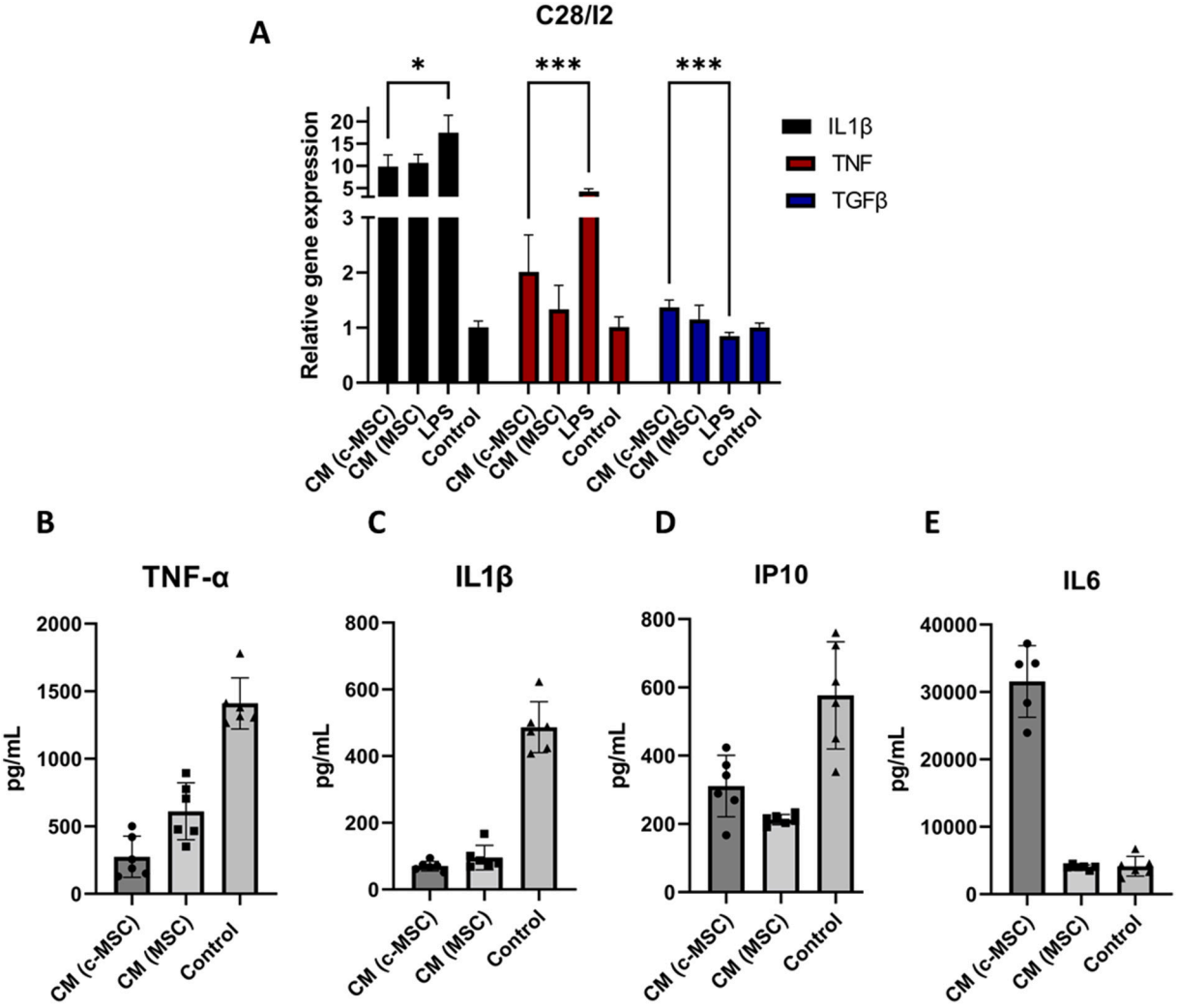

Fig. 4. Comparing the immunomodulatory properties of the c-MSCs and MSCs on stimulated cells. (A) The effect of the conditioned media (CM) from c-MSCs and MSCs on the LPS stimulated C28/I2 chondrocytes. Statistics done using Anova. *P < 0.05, ***P < 0.001 (n = 6) The effect of the CM of c-MSCs and MSCs on the M1 polarized THP1 cells was measured by analyzing the levels of (B) TNFα (C) IL1β (D) IP10 and (E) IL6.

as anti-inflammatory roles [47]. Interestingly, we observed a drastic increase in the production of IL6 (~315 ng/mL with CM of c-MSCs; ~4 ng/mL with CM of MSCs; and ~4.1 ng/mL in control THP1), when the conditioned medium of the c-MSCs were added to the M1 like THP1 cells (Fig. 4E). The conditioned medium from the uncoated MSCs had similar levels of IL6 secretion when compared to the control THP1 cells. The increase in the IL6 secretion with the conditioned medium of the c-MSCs could be due to the sparse amount of gelatin from the H/G coats of the c-MSCs. It has been reported that gelatin in lower concentrations can stimulate the release of IL6 which facilitate muscle regeneration [48]. We believe that a net sum of inflammatory cytokines determines the phenotype of the polarized macrophages, therefore, the reduction of the proinflammatory TNFα, as well as the IL1β and IP10, seen in the THP1 cells could signify the suppression of proinflammatory characteristics of the cells. Furthermore, there have been reports that when the IL6 acts in a pro-inflammatory role, it is at most times in synergy with TNFα [48]. This further strengthens our conviction that IL6 released when the conditioned medium of the c-MSCs is exposed to the M1-like macrophages could play an anti-inflammatory role. Thus, the immunoresponsive properties of the c-MSCs clearly show that the polyelectrolyte coating of the MSCs does not hinder the paracrine signaling capabilities and retains the immunomodulatory functions of the MSCs.

3.4. Differentiation potential of the MSCs

Next, we investigated if the polyelectrolyte coating influences the differentiation abilities of the MSCs. When MSCs are implanted in the myocardial infarction site, it is reported to differentiate into cardiomyocytes in mice myocardial infraction models [49]. Therefore, to evaluate the differentiation potentials of the c-MSCs and the uncoated MSCs, we cultured the cells in osteogenic and adipogenic conditions for a period of two weeks. We also included a group where the c-MSCs and uncoated MSCs were grown in basal medium for two weeks. To analyze the osteogenic differentiation potential, the cells were stained with alizarin red stain. We observed a similar amount of calcium deposits in the c-MSCs and uncoated MSCs cultured under osteogenic conditions (Fig. 5B, C). On the contrary, the c-MSCs and uncoated MSCs in the basal medium did not show any significant calcium deposits (Fig. 5A, D). We further verified the differentiation ability of these cells by quantifying the mRNA levels of the two key osteogenic markers, *alpl* and *bglap*. We

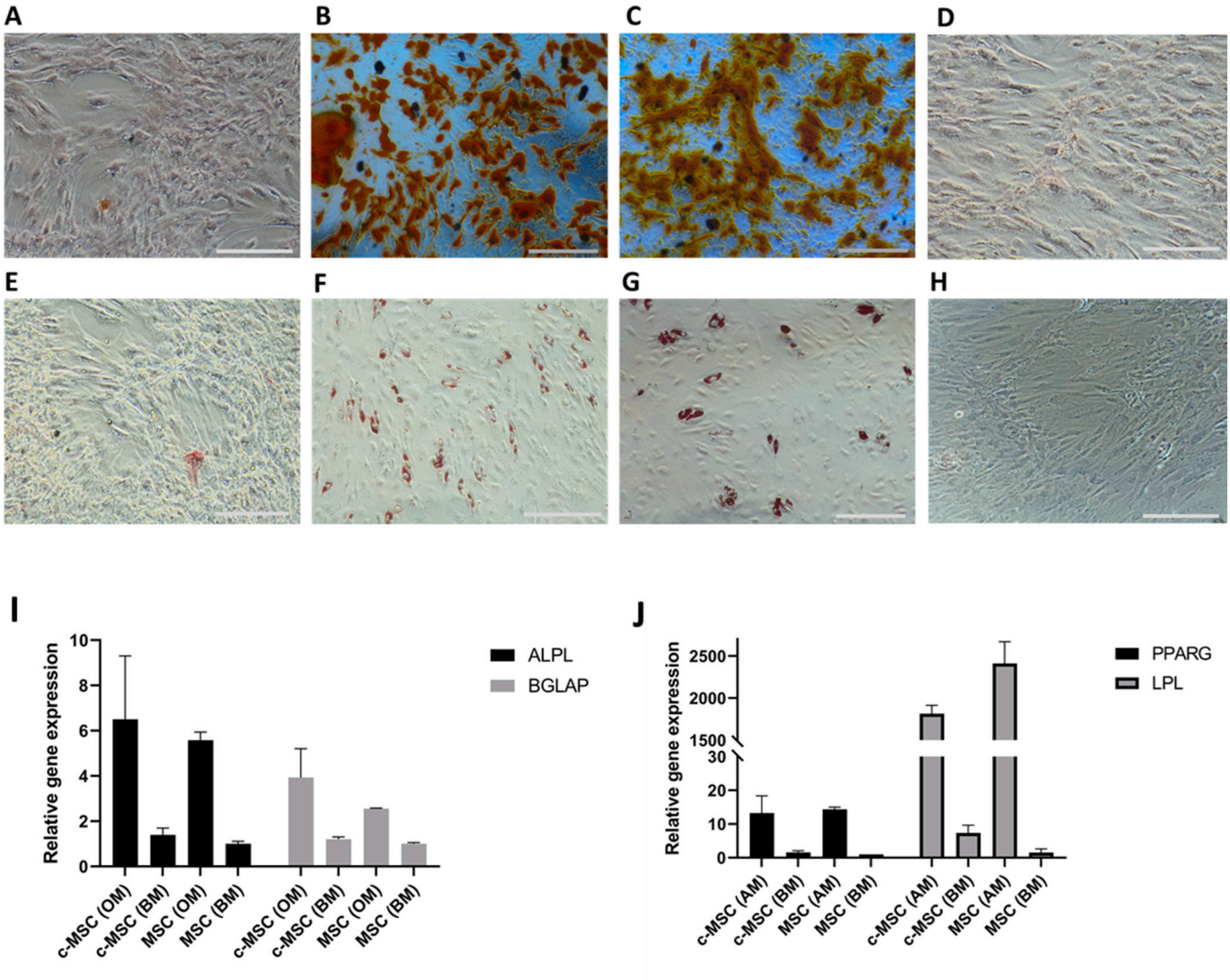

Fig. 5. Differentiation potential of the c-MSCs and uncoated MSCs. Alizarin red staining was used to stain the calcium deposits formed in (A) c-MSCs in basal medium, (B) c-MSCs in osteogenic medium, (C) Uncoated MSCs in osteogenic medium, and (D) uncoated MSCs in basal medium. Oil red S stain was used to stain the lipids present in (E) c-MSCs in basal medium, (F) c-MSCs in adipogenic medium, (G) Uncoated MSCs in adipogenic medium, and (H) uncoated MSCs in basal medium. mRNA levels of (I) osteogenic markers and (J) adipogenic markers (n = 3). OM = osteogenic medium, BM = basal medium, AM = adipogenic medium. Scale 500 μm.

observed similar increase in the *bglap* and *alpl* in the c-MSCs and uncoated MSCs under osteogenic conditions when compared to their respective groups in the basal medium (BM) (Fig. 5I). To analyze the adipogenic differentiation, the cells were cultured under adipogenic conditions and stained with oil red S stain which would stain the lipid present in the cells. These experiments did not reveal any significant differences in the adipogenic differentiation between the c-MSCs and uncoated MSCs (Fig. 5F, G). The c-MSCs and uncoated MSCs did not show any adipogenic differentiation in the basal medium conditions (Fig. 5E, H). Subsequently, we analyzed the mRNA levels of the adipogenic markers (*pparg*, *lpl*) in the c-MSCs and uncoated MSCs. The mRNA levels correlated with the oil red S stain results and elevated levels of *pparg* and *lpl* were observed in the c-MSCs and uncoated MSCs in adipogenic conditions when compared to the cells grown under basal medium conditions (Fig. 5J). These results taken together show that the polyelectrolyte coating of the MSCs does not hinder the differentiation potential of the MSCs.

4. Conclusions

In conclusion, we have designed an unembellished method of protecting the MSCs from the innate immune system, while retaining the functional characteristics and cell proliferation. The MSCs coated with gelatin and heparin in an LbL fashion formed stable nanocapsules around the cells that provided the immunoisolation needed to prevent immune rejection for successful transplantation in patients. The c-MSCs did not trigger the coagulation and complement cascade as evidenced by lower platelet aggregation and suppression of complement (lower C3a and sC5b9) and coagulation cascade (lower TAT complex) activation mediated by the cells. The polyelectrolyte coating on c-MSCs did not hinder their paracrine signaling functions as the conditioned medium of the c-MSCs was able to suppress inflammation in inflamed chondrocytes as well as M1 activated macrophages. Finally, we also demonstrated that the differentiation potential of the c-MSCs was also similar to the uncoated MSCs as we observed in the differentiation studies. Thus, we achieved our ambition of designing a multifunctional cell coating strategy that would mitigate the thrombogenic risks associated with the infusion of MSCs without compromising on their therapeutic function and augment their in-vivo survival as the c-MSCs will be protected from complement attack.

CRediT authorship contribution statement

O. P. Oommen: Conceptualization, Methodology, Writing, Reviewing and editing, Supervision. **V.K. Rangasami**: Data curation, In-vitro studies, Writing, Reviewing and editing, Data analysis. **Kenta Asawa**: Data curation, Hematological studies. **Yuji Teramura**: Hematological studies, Supervision. **Katrina Le Blanc**: Stem cell isolation, and stem cell studies, Supervision. **Bo Nilsson**: Hematological Studies, Reviewing and editing. **Jöns Hilborn**: Reviewing and editing. **Oommen P. Varghese**: Reviewing and editing.

Declaration of competing interest

The authors declare that they have no known competing financial interests or personal relationships that could have appeared to influence the work reported in this paper.

Data availability

Data will be made available on request.

Acknowledgments

The authors would like to thank Dr. Lindsay Davies, Karolinska Institute for her suggestions and expert assistance during the early stages of the project. The authors would also like to thank BioVis, Uppsala University for their assistance in electron microscopy. The authors would also like to acknowledge Swedish Foundation for Strategic Research; project SBE13-0028 “Strategies for stem cell survival” and Swedish Strategic Research ‘StemTherapy’ (Dnr 2009-1035) for their financial assistance.

Appendix A. Supplementary data

Supplementary data to this article can be found online at https://doi.org/10.1016/j.bioadv.2023.213331.

References

[1] B. Lo, L. Parham, Ethical issues in stem cell research, Endocr. Rev. 30 (2009) 204, https://doi.org/10.1210/ER.2008-0031.
[2] D.A. Prentice, Adult stem cells: successful standard for regenerative medicine, Circ. Res. 124 (2019) 837–839, https://doi.org/10.1161/CIRCRESAHA.118.313664.
[3] K. Tatsumi, K. Ohashi, Y. Matsubara, A. Kohori, T. Ohno, H. Kakidachi, A. Horii, K. Kanegae, R. Utoh, T. Iwata, T. Okano, Tissue factor triggers procoagulation in transplanted mesenchymal stem cells leading to thromboembolism, Biochem. Biophys. Res. Commun. 431 (2013) 203–209, https://doi.org/10.1016/J.BBRC.2012.12.134.
[4] G. Moll, J.A. Ankrum, J. Kamhieh-Milz, K. Bieback, O. Ringdén, H.D. Volk, S. Geissler, P. Reinke, Intravascular mesenchymal stromal/stem cell therapy product diversification: time for new clinical guidelines, Trends Mol. Med. 25 (2019) 149–163, https://doi.org/10.1016/j.molmed.2018.12.006.
[5] Y. Li, F. Lin, Mesenchymal stem cells are injured by complement after their contact with serum, Blood 120 (2012) 3436, https://doi.org/10.1182/BLOOD-2012-03-420612.
[6] V.K. Rangasami, G. Nawale, K. Asawa, S. Kadekar, S. Samanta, B. Nilsson, K. N. Ekdahl, S. Miettinen, J. Hilborn, Y. Teramura, O.P. Varghese, O.P. Oommen, Pluronic micelle-mediated tissue factor silencing enhances hemocompatibility, stemness, differentiation potential, and paracrine signaling of mesenchymal stem cells, Biomacromolecules 22 (2021) 1980–1989, https://doi.org/10.1021/ACS.BIOMAC.1C00070/SUPPL_FILE/BM1C00070_SI_001.PDF.
[7] S. Asif, K.N. Ekdahl, K. Fromell, E. Gustafson, A. Barbu, K. le Blanc, B. Nilsson, Y. Teramura, Heparinization of cell surfaces with short peptide-conjugated PEG-lipid regulates thromboinflammation in transplantation of human MSCs and hepatocytes, Acta Biomater. 35 (2016) 194–205, https://doi.org/10.1016/J.ACTBIO.2016.02.018.
[8] G. Song, Y. Hu, Y. Liu, R. Jiang, Layer-by-layer heparinization of the cell surface by using heparin-binding peptide functionalized human serum albumin, Materials 11 (2018) 849, https://doi.org/10.3390/MA11050849, 2018, Vol. 11, Page 849.
[9] Y. Teramura, S. Asif, K.N. Ekdahl, E. Gustafson, B. Nilsson, Cell adhesion induced using surface modification with cell-penetrating peptide-conjugated Poly(ethylene glycol)-lipid: a new cell glue for 3D cell-based structures, ACS Appl. Mater. Interfaces 9 (2017) 244–254, https://doi.org/10.1021/ACSAMI.6B14584/SUPPL_FILE/AM6B14584_SI_001.PDF.
[10] L. Zhang, G. Liu, K. Lv, J. Xin, Y. Wang, J. Zhao, W. Hu, C. Xiao, K. Zhu, L. Zhu, J. Nan, Y. Feng, H. Zhu, W. Chen, W. Zhu, J. Zhang, J. Wang, B. Wang, X. Hu, Surface-anchored nanogel coating endows stem cells with stress resistance and reparative potency via turning down the cytokine-receptor binding pathways, Adv. Sci. 8 (2021), https://doi.org/10.1002/advs.202003348.
[11] N.G. Veerabadran, P.L. Goli, S.S. Stewart-Clark, Y.M. Lvov, D.K. Mills, Nanoencapsulation of stem cells within polyelectrolyte multilayer shells, Macromol. Biosci. 7 (2007) 877–882, https://doi.org/10.1002/MABI.200700061.
[12] H. Peng, L. Chelvarajan, R. Donahue, A. Gottipati, C.F. Cahall, K.A. Davis, H. Tripathi, A. Al-Darraji, E. Elsawalhy, N. Dobrozsi, A. Srinivasan, B.M. Levitan, R. Kong, E. Gao, A. Abdel-Latif, B.J. Berron, Polymer cell surface coating enhances mesenchymal stem cell retention and cardiac protection, ACS Appl. Bio Mater. 4 (2021) 1655–1667, https://doi.org/10.1021/ACSABM.0C01473/SUPPL_FILE/MT0C01473_SI_001.PDF.
[13] K. Asawa, K. Ishihara, K.N. Ekdahl, B. Nilsson, Y. Teramura, K. Asawa, Y. Teramura, K. Ishihara, K.N. Ekdahl, B. Nilsson, Cell surface functionalization with heparin-conjugated lipid to suppress blood activation, Adv. Funct. Mater. 31 (2021), 2008167, https://doi.org/10.1002/ADFM.202008167.
[14] P.H. Nilsson, K.N. Ekdahl, P.U. Magnusson, H. Qu, H. Iwata, D. Ricklin, J. Hong, J. D. Lambris, B. Nilsson, Y. Teramura, Autoregulation of thromboinflammation on biomaterial surfaces by a multicomponent therapeutic coating, Biomaterials 34 (2013) 985–994, https://doi.org/10.1016/J.BIOMATERIALS.2012.10.040.
[15] J. Zeng, M. Matsusaki, Layer-by-layer assembly of nanofilms to control cell functions, Polym. Chem. 10 (2019) 2960–2974, https://doi.org/10.1039/C9PY00305C.
[16] G. Liu, L. Li, D. Huo, Y. Li, Y. Wu, L. Zeng, P. Cheng, M. Xing, W. Zeng, C. Zhu, A VEGF delivery system targeting MI improves angiogenesis and cardiac function based on the tropism of MSCs and layer-by-layer self-assembly, Biomaterials 127 (2017) 117–131, https://doi.org/10.1016/j.biomaterials.2017.03.001.
[17] W. Li, T. Guan, X. Zhang, Z. Wang, M. Wang, W. Zhong, H. Feng, M. Xing, J. Kong, The effect of layer-by-layer assembly coating on the proliferation and differentiation of neural stem cells, ACS Appl. Mater. Interfaces 7 (2015) 3018–3029, https://doi.org/10.1021/am504456t.

[18] L.P.B. Guerzoni, Y. Tsukamoto, D.B. Gehlen, D. Rommel, T. Haraszti, M. Akashi, L. de Laporte, A layer-by-layer single-cell coating technique to produce injectable beating mini heart tissues via microfluidics, Biomacromolecules 20 (2019) 3746–3754, https://doi.org/10.1021/ACS.BIOMAC.9B00786/SUPPL_FILE/BM9B00786_SI_001.ZIP.
[19] C. Gravastrand, S. Hamad, H. Fure, B. Steinkjer, L. Ryan, J. Oberholzer, J. D. Lambris, I. Lacík, T.E. Mollnes, T. Espevik, O.L. Brekke, A.M. Rokstad, Alginate microbeads are coagulation compatible, while alginate microcapsules activate coagulation secondary to complement or directly through FXII, Acta Biomater. 58 (2017) 158–167, https://doi.org/10.1016/j.actbio.2017.05.052.
[20] A.B. Bello, D. Kim, D. Kim, H. Park, S.H. Lee, Engineering and functionalization of gelatin biomaterials: from cell culture to medical applications, Tissue Eng. B Rev. 26 (2020) 164–180, https://doi.org/10.1089/TEN.TEB.2019.0256/ASSET/IMAGES/LARGE/TEN.TEB.2019.0256_FIGURE4.JPEG.
[21] A.R. Donaldson, C.E. Tanase, D. Awuah, P.V. Bathrinarayanan, L. Hall, M. Nikkhah, A. Khademhosseini, F. Rose, C. Alexander, A.M. Ghaemmaghami, Photocrosslinkable gelatin hydrogels modulate the production of the major pro-inflammatory cytokine, TNF-α, by human mononuclear cells, Front. Bioeng. Biotechnol. 6 (2018) 116, https://doi.org/10.3389/FBIOE.2018.00116/BIBTEX.
[22] C. Page, Heparin and related drugs: beyond anticoagulant activity, ISRN Pharmacol. 2013 (2013) 1–13, https://doi.org/10.1155/2013/910743.
[23] T. Ahmed, J. Garrigo, I. Danta, Preventing bronchoconstriction in exercise-induced asthma with inhaled heparin, N. Engl. J. Med. 329 (1993) 90–95, https://doi.org/10.1056/NEJM199307083290204.
[24] F. Redini, J.M. Tixier, M. Petitou, J. Choay, L. Robert, W. Hornebeck, Inhibition of leucocyte elastase by heparin and its derivatives, Biochem. J. 252 (1988) 515–519, https://doi.org/10.1042/BJ2520515.
[25] M.M. Teixeira, A.G. Rossi, P.G. Hellewell, Adhesion mechanisms involved in C5a-induced eosinophil homotypic aggregation, J. Leukoc. Biol. 59 (1996) 389–396, https://doi.org/10.1002/JLB.59.3.389.
[26] V. Evangelista, P. Piccardoni, N. Maugeri, G. de Gaetano, C. Cerletti, Inhibition by heparin of platelet activation induced by neutrophil-derived cathepsin G, Eur. J. Pharmacol. 216 (1992) 401–405, https://doi.org/10.1016/0014-2999(92)90437-9.
[27] J.M.F. Chacon, M.L.M. de Andrea, L. Blanes, L.M. Ferreira, Effects of topical application of 10,000 IU heparin on patients with perineal dermatitis and second-degree burns treated in a public pediatric hospital, J. Tissue Viability 19 (2010) 150–158, https://doi.org/10.1016/J.JTV.2010.03.003.
[28] S. Samanta, V. le Joncour, O. Wegrzyniak, V.K. Rangasami, H. Ali-Löytty, T. Hong, R.K. Selvaraju, O. Aberg, J. Hilborn, P. Laakkonen, O.P. Varghese, O. Eriksson, H. Cabral, O.P. Oommen, Heparin-derived theranostic nanoprobes overcome the blood–brain barrier and target glioma in murine model, Adv. Ther. (Weinh.) (2022), 2200001, https://doi.org/10.1002/adtp.202200001.
[29] A. Nilasaroya, P.J. Martens, J.M. Whitelock, Enzymatic degradation of heparin-modified hydrogels and its effect on bioactivity, Biomaterials 33 (2012) 5534–5540, https://doi.org/10.1016/J.BIOMATERIALS.2012.04.022.
[30] A. Meirovitz, R. Goldberg, A. Binder, A.M. Rubinstein, E. Hermano, M. Elkin, Heparanase in inflammation and inflammation-associated cancer, FEBS J. 280 (2013) 2307–2319, https://doi.org/10.1111/FEBS.12184.
[31] T.R. Donahue, J.R. Hiatt, R.W. Busuttil, Collagenase and surgical disease, Hernia 10 (2006) 478–485, https://doi.org/10.1007/S10029-006-0146-7.
[32] A. Fakhardo, E. Anastasova, V. Makarov, E. Ikonnikova, E. Kulko, N. Agadzhanian, M. Yakunina, L. Shkodenko, S. Tsvetikova, M. Toropko, E. Koshel, M. Zakharov, G. Alexandrov, O. Khuttunen, P. Kulikov, O. Burmistrov, V. Vinogradov, A. Prilepskii, Heparin-coated iron oxide nanoparticles: application as a liver contrast agent, toxicity and pharmacokinetics, J. Mater. Chem. B 10 (2022) 7797–7807, https://doi.org/10.1039/D2TB00759B.
[33] A. Susanto, B.W. Putera, A. Wijaya, A. Muhtadi, Effect of heparin on proliferation mesencymal stem cell, Cytotherapy 21 (2019) S87–S88, https://doi.org/10.1016/j.jcyt.2019.03.515.
[34] H. Lee, N.R. Han, J.Y. Hwang, J.I. Yun, C. Kim, K.H. Park, S.T. Lee, Gelatin directly enhances neurogenic differentiation potential in bone marrow-derived mesenchymal stem cells without stimulation of neural progenitor cell proliferation, DNA Cell Biol. 35 (2016) 530–536, https://doi.org/10.1089/dna.2016.3237.
[35] H. Yu, E.M. Muñoz, R.E. Edens, R.J. Linhardt, Kinetic studies on the interactions of heparin and complement proteins using surface plasmon resonance, Biochim. Biophys. Acta Gen. Subj. 1726 (2005) 168–176, https://doi.org/10.1016/J.BBAGEN.2005.08.003.
[36] A. Zaferani, D. Talsma, M.K.S. Richter, M.R. Daha, G.J. Navis, M.A. Seelen, J. van den Born, Heparin/heparan sulphate interactions with complement—a possible target for reduction of renal function loss? Nephrol. Dial. Transplant. 29 (2014) 515–522, https://doi.org/10.1093/NDT/GFT243.
[37] B.Z. Johnson, A.W. Stevenson, C.M. Prêle, M.W. Fear, F.M. Wood, The role of IL-6 in skin fibrosis and cutaneous wound healing, Biomedicines 8 (2020), https://doi.org/10.3390/BIOMEDICINES8050101.
[38] H.O. Rennekampff, J.F. Hansbrough, V. Kiessig, C. Doré, M. Sticherling, J. M. Schröder, Bioactive interleukin-8 is expressed in wounds and enhances wound healing, J. Surg. Res. 93 (2000) 41–54, https://doi.org/10.1006/jsre.2000.5892.
[39] R. Zhang, J. Ma, J. Han, W. Zhang, J. Ma, Mesenchymal stem cell related therapies for cartilage lesions and osteoarthritis, Am. J. Transl. Res. 11 (2019) 6275. /pmc/articles/PMC6834499/ (accessed March 31, 2022).
[40] Y.I.Ng Li, B.W. Ang, G. Li, SendOrders for Reprintsto reprints@benthamscience.net the roles of mesenchymal stem cells in tissue repair and disease modification, Curr. Stem Cell Res. Ther. 9 (2014) 424–431.
[41] S.L. Stubbs, S.T.F. Hsiao, H.M. Peshavariya, S.Y. Lim, G.J. Dusting, R.J. Dilley, Hypoxic preconditioning enhances survival of human adipose-derived stem cells and conditions endothelial cells in vitro, Stem Cells Dev. 21 (2012) 1887–1896, https://doi.org/10.1089/SCD.2011.0289/ASSET/IMAGES/LARGE/FIGURE6.JPEG.
[42] J.R.K. Samal, V.K. Rangasami, S. Samanta, O.P. Varghese, O.P. Oommen, Discrepancies on the role of oxygen gradient and culture condition on mesenchymal stem cell fate, Adv. Healthc. Mater. 10 (2021), 2002058, https://doi.org/10.1002/adhm.202002058.
[43] Q. Ge, H. Zhang, J. Hou, L. Wan, W. Cheng, X. Wang, D. Dong, C. Chen, J. Xia, J. Guo, X. Chen, X. Wu, VEGF secreted by mesenchymal stem cells mediates the differentiation of endothelial progenitor cells into endothelial cells via paracrine mechanisms, Mol. Med. Rep. 17 (2018) 1667, https://doi.org/10.3892/MMR.2017.8059.
[44] K. English, J.M. Ryan, L. Tobin, M.J. Murphy, F.P. Barry, B.P. Mahon, Cell contact, prostaglandin E2 and transforming growth factor beta 1 play non-redundant roles in human mesenchymal stem cell induction of CD4+CD25Highforkhead box P3+ regulatory T cells, Clin. Exp. Immunol. 156 (2009) 149–160, https://doi.org/10.1111/J.1365-2249.2009.03874.X.
[45] J.H. Dufour, M. Dziejman, M.T. Liu, J.H. Leung, T.E. Lane, A.D. Luster, IFN-γ-inducible protein 10 (IP-10; CXCL10)-deficient mice reveal a role for IP-10 in effector T cell generation and trafficking, J. Immunol. 168 (2002) 3195–3204, https://doi.org/10.4049/JIMMUNOL.168.7.3195.
[46] S. Liu, F. Liu, Y. Zhou, B. Jin, Q. Sun, S. Guo, Immunosuppressive property of MSCs mediated by cell surface receptors, Front. Immunol. 11 (2020) 1076, https://doi.org/10.3389/fimmu.2020.01076.
[47] G. Casella, L. Garzetti, A.T. Gatta, A. Finardi, C. Maiorino, F. Ruffini, G. Martino, L. Muzio, R. Furlan, IL4 induces IL6-producing M2 macrophages associated to inhibition of neuroinflammation in vitro and in vivo, J. Neuroinflammation 13 (2016) 1–10, https://doi.org/10.1186/S12974-016-0596-5/FIGURES/6.
[48] X. Liu, E. Zu, X. Chang, X. Ma, Z. Wang, X. Song, X. Li, Q. Yu, K.I. Kamei, T. Hayashi, K. Mizuno, S. Hattori, H. Fujisaki, T. Ikejima, D.O. Wang, Bi-phasic effect of gelatin in myogenesis and skeletal muscle regeneration, Dis. Model. Mech. 14 (2021), https://doi.org/10.1242/dmm.049290.
[49] D. Orlic, J. Kajstura, S. Chimenti, D.M. Bodine, A. Leri, P. Anversa, Bone marrow stem cells regenerate infarcted myocardium, Pediatr. Transplant. 7 (Suppl. 3) (2003) 86–88, https://doi.org/10.1034/J.1399-3046.7.S3.13.X.